

# Evaluation of the intermediates generated during the degradation of Diuron and Linuron herbicides by the photo-Fenton reaction

María José Farré<sup>a</sup>, Stephan Brosillon<sup>b</sup>, Xavier Domènech<sup>a</sup>, José Peral<sup>a,\*</sup>

<sup>a</sup> *Departament de Química, Universitat Autònoma de Barcelona, 08193 Bellaterra, Spain*

<sup>b</sup> *Laboratoire Rennais de Chimie et Ingénierie des Procédés, Ecole Nationale Supérieure de Chimie de Rennes, Avenue du Général Leclerc, 3700 Rennes, France*

Received 7 December 2006; received in revised form 26 February 2007; accepted 26 February 2007

Available online 3 March 2007

## Abstract

Freshwater polluted with herbicides is a problem of general concern since these compounds are commonly toxic and non-biodegradable. An innovative technology for the elimination of such compounds is the coupling between an Advanced Oxidation Process (AOP) and a biological treatment. The success of this coupled methodology depends on the biodegradable nature of the by-products originated at the end of the chemical stage. The present paper is based on the analysis of the intermediates generated during the chemical oxidation of Diuron and Linuron herbicides using three different doses of photo-Fenton reactants. Among the three effluents obtained after the chemical pre-treatment, only the most oxidised is completely biodegradable. Several analytical methods: reverse phase ultra pressure liquid chromatography UPLC(RP)/MS, ionic chromatography IC and gas chromatography/MS have been used to elucidate the degradation mechanism. Beyond conventional separation methods, hydrophilic interaction chromatography HILIC coupled with mass spectrometry has been necessary to identify small polar compounds at the end of oxidation process. The first steps of the degradation mechanism have been ascertained. Furthermore, different by-products have been found at the end of the chemical process when different reactant doses were used. These differences have been based on the presence of urea derivates (methyurea, 1,1-dimethylurea) and unidentified chlorinated compounds.

© 2007 Elsevier B.V. All rights reserved.

**Keywords:** Biodegradability; Herbicides; By-products; Biological treatment; photo-Fenton

## 1. Introduction

Nowadays herbicides are indispensable for agricultural practices. Nevertheless herbicides also represent a water quality risk factor because these substances are generally toxic and non-biodegradable. A part from lixivates coming from agricultural fields, washing of herbicide containers and unused treatment solutions also contribute to this problem producing highly polluted effluents that should be treated before their disposal to the environment.

Conventional technologies for the removal of pollutants include biological, physical and chemical treatments. The drawbacks of biological wastewater treatment plants (WWTP) are based on the requirement of a long residence time to degrade the pollutants because microorganisms are affected by the toxicity of

the herbicides [1]. Physical treatments require a post-treatment to remove the pollutant from the newly contaminated environment. Finally, chemical treatments require a large amount of reactant and generally are expensive. In this situation, the development of new technologies aimed at the straightforward degradation of such substances is of practical interest. In recent years the coupling between an Advanced Oxidation Process (AOP) and biological systems for the treatment of different polluted effluents has been proposed [2–7]. In this way the AOP is performed as a first step to enhance the biodegradability and generate a new effluent able to be treated in a biological plant.

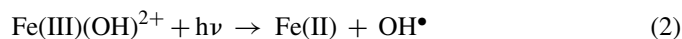
AOPs are based on the production of the highly reactive hydroxyl radical (OH<sup>•</sup>) under mild experimental conditions. This radical can react with organic matter (redox standard potential 2.8 V *versus* NHE) producing CO<sub>2</sub> as final product. Due to the reactivity of free hydroxyl radicals, their attack is non-selective, which is useful for the treatment of wastewater containing many different pollutants.

\* Corresponding author. Tel.: +34 93 581 2772; fax: +34 93 581 2920.  
E-mail address: [jose.peral@uab.es](mailto:jose.peral@uab.es) (J. Peral).

Photo-Fenton is preferred among the other AOPs because it achieves high reaction yields with low treatment costs, mainly due to the possibility of a more effective use of solar light as a photon source [8]. In this process the hydroxyl radical promoters are Fe(II) and hydrogen peroxide [9] (reaction 1, Fenton process).



Under irradiation of  $\lambda < 410$  nm, Fe(III) can be reduced to Fe(II) closing a loop mechanism where Fe species act as catalyst, giving rise to additional  $\text{OH}^\bullet$  [10] (reaction 2, photo-Fenton process).



The best optimization of a chemical–biological coupled system can be achieved by using a low amount of reactants in the chemical step. However, these reactant doses should assure the biocompatibility of the by-products generated. With this objective, the monitoring of the intermediates produced in the chemical treatment is indispensable to understand the biological compatibility of the phototreated effluent. This monitoring is not always easy since by-products generated in such oxidation processes can be small polar compounds with different chemical structure and low concentration. In this situation, reversed phase liquid chromatography HPLC (RP) is not the best separation method because polar compounds are not retained on non-polar stationary phases. On the other hand, normal phase HPLC eluents (often based on hexane) produce an incompatibility with mass detectors since ionization is not easily achieved in totally organic, non-polar eluents. When hydrophilic interaction chromatography (HILIC) [11] is performed aqueous mobile phases, usually containing more than 50% of organic solvent, and a polar stationary phase like diol, silica or amine are used. The retention of polar compounds is increased when the proportion of organic solvent is increased.

Alpert et al. [11] suggested that the retention mechanism involves portioning of the analyte between the mobile phase and a layer of mobile phase enriched with water on the stationary phase. In this way the elution order in HPLC(HILIC) is more or less the opposite of that seen in HPLC (RP). So HPLC (HILIC) coupled with mass spectrometer appears to be an appropriate method for the determination of the concentration and structure of small polar compounds.

Phenylurea compounds are herbicides which have been widely used since their discovery in 1950. Linuron, 3-[3,4-(dichlorophenyl)-1-methoxy-1-methylurea] and Diuron 3-[3,4-(dichlorophenyl)-1,1-dimethylurea] were selected as target compounds. The degradation of Diuron and Linuron herbicides by means of the coupling of photo-Fenton and biological treatment was performed and published in a previous work [5]. In that study, three different photo-Fenton reagent doses were used in the chemical treatment (i.e., A:  $[\text{Fe(II)}]=9.25 \text{ mg L}^{-1}$ ,  $[\text{H}_2\text{O}_2]=97.1 \text{ mg L}^{-1}$ ; B:  $[\text{Fe(II)}]=13.3 \text{ mg L}^{-1}$ ,  $[\text{H}_2\text{O}_2]=143 \text{ mg L}^{-1}$ ; C:  $[\text{Fe(II)}]=15.9 \text{ mg L}^{-1}$ ,  $[\text{H}_2\text{O}_2]=202 \text{ mg L}^{-1}$ ). The photo-Fenton reaction was run for 60 min. The disappearance of initial herbicides

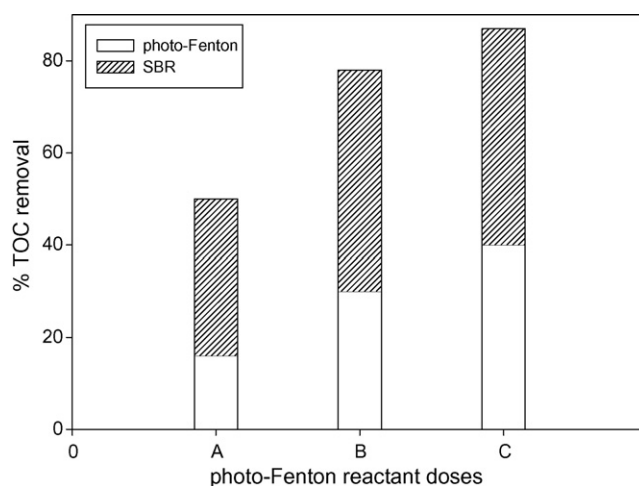


Fig. 1. Percent (%) TOC removal in photo-Fenton pre-treatment and biological sequencing batch reactor (SBR) coupling system as function of photo-Fenton dose. A:  $9.25 \text{ mg L}^{-1}$  Fe(II),  $97.1 \text{ mg L}^{-1}$   $\text{H}_2\text{O}_2$ ; B:  $13.3 \text{ mg L}^{-1}$  Fe(II),  $143 \text{ mg L}^{-1}$   $\text{H}_2\text{O}_2$  and C:  $15.9 \text{ mg L}^{-1}$  Fe(II),  $202 \text{ mg L}^{-1}$   $\text{H}_2\text{O}_2$ .

during the photo-Fenton process was determined by HPLC/UV analyses for all the doses used. The percentages of TOC removal after the chemical step when dose A, B and C were used were 16%, 25% and 36%, respectively. After that, a biological system was used in order to completely remove organic matter from solution. Among the three photo-Fenton doses selected, only dose C successfully converted the initial toxic and non-biodegradable effluent into a new form which was able to be assimilated by the biomass. Fig. 1 shows the percentage of TOC removal after the chemical-biological coupled system for the treatment of Diuron and Linuron.

The aim of the present paper is to enhance the knowledge on the chemical composition of the three effluents after photo-Fenton in view to understand the difference of biodegradability of each effluent as well as to determine a possible reaction mechanism of the oxidation of both herbicides. Heteroatoms, short acids as well as oxidized by-products evolution were analyzed in order to obtain such information.

## 2. Materials and methods

### 2.1. Preparation of initial wastewater

Diuron (98.5% Aragonesas Agro S.A. technical grade) and Linuron (92.6% Makhteshim Agan España, S.A.) were used as target compounds in the experiments. A initial saturated solution was prepared in water purified in a Millipore Milli-Q system and then filtrated by means of a  $20 \mu\text{m}$  nylon filter. The concentration of the initial solution was  $42 \text{ mg L}^{-1}$  and  $75 \text{ mg L}^{-1}$  of Diuron and Linuron, respectively. These values correspond to the maximum solubility of both herbicides in water at  $25^\circ\text{C}$ . The initial solution was transparent and colourless.

### 2.2. Photo-Fenton experimental procedure

$\text{FeSO}_4 \cdot 7\text{H}_2\text{O}$  (Merck) and  $\text{H}_2\text{O}_2$  (Panreac, 33% w/v) were used in the photo-Fenton experiments. Experiments were con-

ducted at  $25 \pm 0.2^\circ\text{C}$  in a cylindrical Pyrex thermostatic cell of  $250\text{ cm}^3$  capacity provided with a magnetic stirrer. A 6W Philips black light with a measured intensity of  $0.21\text{ mW/cm}^2$  was used as a photon source. In all the experiments pH was adjusted to 2.8 with  $\text{H}_2\text{SO}_4$ . Three different combinations of photo-Fenton reagents were used (i.e., A:  $[\text{Fe(II)}]=9.25\text{ mg L}^{-1}$ ,  $[\text{H}_2\text{O}_2]=97.1\text{ mg L}^{-1}$ ; B:  $[\text{Fe(II)}]=13.3\text{ mg L}^{-1}$ ,  $[\text{H}_2\text{O}_2]=143\text{ mg L}^{-1}$ ; C:  $[\text{Fe(II)}]=15.9\text{ mg L}^{-1}$ ,  $[\text{H}_2\text{O}_2]=202\text{ mg L}^{-1}$ .)

The experimental procedure was as follows: in each experiment the photo-reactor was charged with 0.250 L of solution to be photo-treated. The pH of these solutions was always adjusted to 2.8 and after that  $\text{FeSO}_4 \cdot 7\text{H}_2\text{O}$  was added. Finally, the hydrogen peroxide was added to the solution and UV light was switched on. The total photo-treatment time selected was 60 min.

### 2.3. Analytical methods

TOC was analyzed with a Shimadzu TOC-VCSH apparatus.  $\text{Cl}^-$  and  $\text{NO}_3^-$  ions were analyzed by Dionex DX120 ion chromatography equipped with a conductivity detector using an IonPac<sup>®</sup> AS19 anion-exchange column ( $4\text{ mm} \times 250\text{ mm}$ ) as the stationary phase. A gradient of KOH in water: 10 mM from 0 to 10 min and then increasing to 45 mM from 10 to 25 min was used as mobile phase. The flow rate was  $1\text{ mL min}^{-1}$  and the injection volume was  $500\text{ }\mu\text{L}$ . The mobile phase was electrolytically generated by means of a EGC II KOH.

For the determination of short acids (oxalic, acetic and formic acids) the same system was used but the gradient was changed: 10 mM from 0 to 10 min and then increasing to 58 mM from 10 to 40 min.

Ammonium was analyzed using an Orion 95-12 Ammonia Electrode and a Crison pH/mV meter with readability to 0.1 mV.

Separation and identification of first oxidation by-products were performed with an Acquity<sup>™</sup> ultra performance LC (Waters), equipped with a mass spectrometer Quattro Premier-Micromass-(Waters). The mobile phase was a mixture of (A) acetonitrile and (B) acetonitrile (10%), water and formic acid (0.1%). The composition of the phase changed according to the following gradient: 20% of A was kept during 4 min. From 4 to 5 min, B was steadily increased to attain the 95%. Finally the phase turned to the initial composition until the end of the run. The system was equipped with a UPLC<sup>™</sup> BEH C<sub>18</sub> capillary column ( $2.1\text{ mm} \times 100\text{ mm} \times 1.7\text{ }\mu\text{m}$ ). Mass spectra were obtained by electro-spray ionization (ESI) in negative mode. Cone voltage of 25 V in full scan mode and 23 V in the MRM mode were used. When samples concentration was required, OASIS HLB 6cc cartridges were used for solid phase extraction and ethanol was used as eluent.

3,4-Dichloroaniline and 3,4-dichlorophenyl isocyanate were identified during photodegradation of both pesticides by means of GC-MS. These products were extracted from the treated solution by solid phase extraction (Maxi-Clean C18 600 mg, Alltech). A mixture of dichloromethane and ethyl acetate (1/1, v/v) was used to elute the intermediate products. This solution was concentrated under nitrogen flow for the analysis of the by-products. The GC-MS was performed using a HP 6890 series

GC equipped with a MS (HP 5973). The system was fitted with a HP-5MS capillary column ( $30 \times 0.25\text{ i.d.} \times 0.25\text{ }\mu\text{m}$ ), splitless injection, and helium was used as carrier gas ( $1\text{ mL min}^{-1}$ ). The GC oven temperature was programmed to initially hold at  $50^\circ\text{C}$  for 3 min, to increase from  $50\text{--}275^\circ\text{C}$  at a rate of  $5^\circ\text{C min}^{-1}$  and to hold at  $275^\circ\text{C}$  for 15 min. The injector and interface temperature were kept at  $250^\circ\text{C}$ . Mass spectra were obtained by electron-impact (EI) in negative mode at 70 eV, using scan mode ( $30\text{--}800\text{ m/z}$ ).

Small polar compounds were analysed with a HPLC (HILIC) coupled with a Esquire 3000 (Bruker) mass spectrometer, using an Agilent 1100 liquid chromatograph equipped with a Nucleosil diol column ( $7\text{ }\mu\text{m}, 15\text{ cm} \times 0.4\text{ cm}$ ). The injection volume was  $5.00\text{ }\mu\text{L}$  and temperature was not controlled. The mobile phase consisted of (A) acetonitrile and (B) 20 mM aqueous ammonium formate, the pH of which was adjusted to 3.3 with formic acid. The composition of the phase changed following a gradient: 95% of A was kept during 3 min, then it changed from 95% to 50% of A in three more minutes, steady decrease to 20% of A up to minute 10. From 10 to 14 min the composition was kept stable at 20% A. Finally from 14 to 30 min the mobile phase was returned to initial conditions. Electro-spray (ESI) in positive mode was used for detection. The capillary voltage was optimized to 5000 V using full scan mode ( $50\text{--}200\text{ m/z}$ ).

## 3. Results and discussion

### 3.1. Heteroatoms evolution

Mineralization of Diuron and Linuron herbicides, using A, B and C photo-Fenton reactant dose, was followed by means of TOC measurements over 150 min (see Fig. 2 for relative TOC abatement). The mineralization rate did not follow simple first or zero-order kinetics models and overall reaction rate constants could not be estimated. The complexity of the data is due to the fact that TOC is a parameter which is often the consequence of

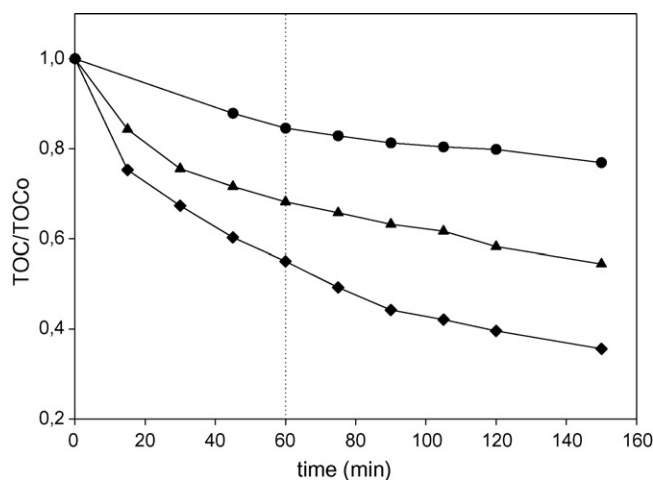


Fig. 2. Relative TOC evolution vs. irradiation time with A (●), B (▲) and C (◆) reagent doses for Diuron and Linuron herbicides. A:  $9.25\text{ mg L}^{-1}\text{ Fe(II)}$ ,  $97.1\text{ mg L}^{-1}\text{ H}_2\text{O}_2$ ; B:  $13.3\text{ mg L}^{-1}\text{ Fe(II)}$ ,  $143\text{ mg L}^{-1}\text{ H}_2\text{O}_2$  and C:  $15.9\text{ mg L}^{-1}\text{ Fe(II)}$ ,  $202\text{ mg L}^{-1}\text{ H}_2\text{O}_2$ . pH 2.8,  $T=25^\circ\text{C}$ .

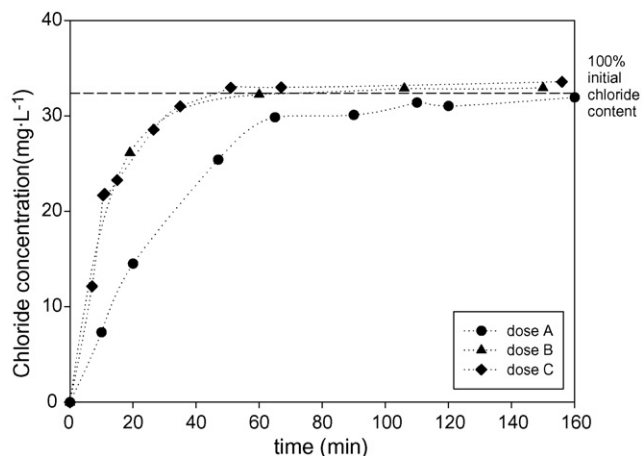
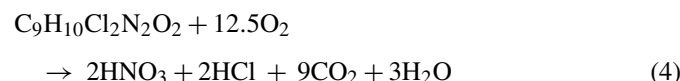
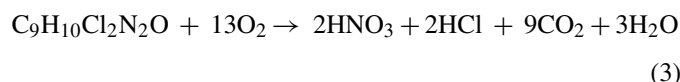


Fig. 3. Chloride concentration vs. irradiation time with A, B and C reagent doses for Diuron and Linuron herbicides. A:  $9.25 \text{ mg L}^{-1} \text{ Fe(II)}$ ,  $97.1 \text{ mg L}^{-1} \text{ H}_2\text{O}_2$ ; B:  $13.3 \text{ mg L}^{-1} \text{ Fe(II)}$ ,  $143 \text{ mg L}^{-1} \text{ H}_2\text{O}_2$  and C:  $15.9 \text{ mg L}^{-1} \text{ Fe(II)}$ ,  $202 \text{ mg L}^{-1} \text{ H}_2\text{O}_2$ . pH 2.8,  $T=25^\circ\text{C}$ .

the parallel degradation of several compounds. The stoichiometry of the complete mineralization of Diuron and Linuron can be expressed with the following global equations:



It is well known that chlorinated compounds are generally not biodegradable [13], consequently it is important to access the ratio of mineralization of chlorine during irradiation. For that reason, the formation of chloride ion was investigated. Fig. 3 shows chloride evolution when the three selected doses were used. Chloride evolves very quickly suggesting an early degradation/dechlorination stage, as described before [12]. From Fig. 3 it is seen that chlorine was completely removed from the aromatic ring before 60 min in the effluents treated with dose B and C. In both experiments the total amount of  $\text{Cl}^-$  produced at the end of the reaction was approximately  $32.3 \text{ mg L}^{-1}$  (100% of the Diuron and Linuron chlorine content). On the other hand, 7.8% of chlorine remained linked to the aromatic ring after 60 min when dose A was used to treat the polluted effluent. This means that a chlorinated intermediate is present in the residual TOC at the end of the chemical treatment with reagent dose A.

Nitrogen release was monitored by the combination of free ammonia and nitrate. Although the reactions shown above have been written taking into account the most oxidized state, ammonia could be formed and then oxidized to nitrate at long irradiation times. Both, ammonia and nitrate have been detected at different relative concentrations depending on the dose used in the pre-treatment. By observing Fig. 4, it can be concluded that the amount of nitrate and ammonia formed in the oxidation process is directly proportional to the concentration of oxidant used. When dose C was selected (the highest oxidant concentration used in the present study), only 18% of total nitrogen present in the initial molecules was recovered. Incomplete

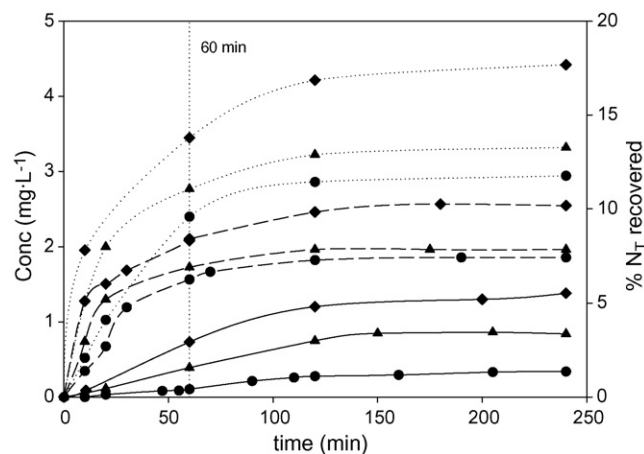


Fig. 4. Nitrate (—), ammonium (---) and total nitrogen recovered (· · ·) evolution vs. irradiation time during the photo-degradation of Diuron and Linuron with A (●), B (▲) and C (◆) reagent doses. A:  $9.25 \text{ mg L}^{-1} \text{ Fe(II)}$ ,  $97.1 \text{ mg L}^{-1} \text{ H}_2\text{O}_2$ ; B:  $13.3 \text{ mg L}^{-1} \text{ Fe(II)}$ ,  $143 \text{ mg L}^{-1} \text{ H}_2\text{O}_2$  and C:  $15.9 \text{ mg L}^{-1} \text{ Fe(II)}$ ,  $202 \text{ mg L}^{-1} \text{ H}_2\text{O}_2$ . pH 2.8,  $T=25^\circ\text{C}$ .

nitrogen mass balance indicates that other nitrogen containing compounds must be present in the solution during the process.

At this point it was necessary to find an analytical technique able to determine this type of compounds dissolved in complex matrixes.

### 3.2. Short organic acids evolution

The evolution of acetic, formic and oxalic acids concentration along 350 min of photo-Fenton oxidation reaction was investigated. As seen in Fig. 5, the concentration of acetic acid increases to reach a maximum after approximately 50 min when dose A was used to oxidized Diuron and Linuron. After 60 min of irradiation, the time used to perform biological coupling, acetic acid concentration was  $4.88 \text{ mg L}^{-1}$ . On the other hand, when doses

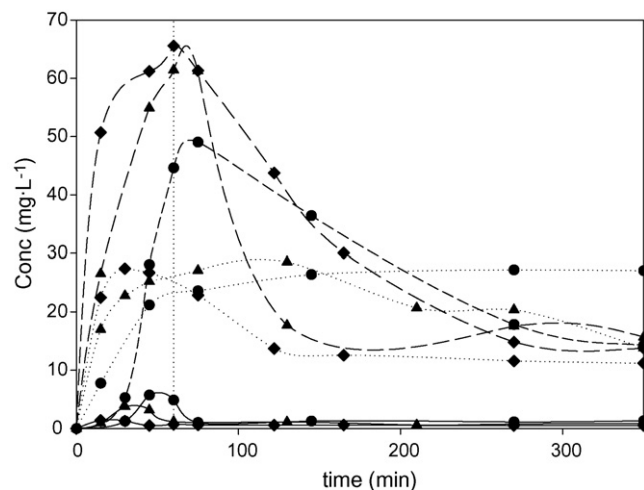


Fig. 5. Acetic acid (—), oxalic acid (---) and formic acid (· · ·) evolution vs. irradiation time during the photo-degradation of Diuron and Linuron with A (●), B (▲) and C (◆) reagent doses. A:  $9.25 \text{ mg L}^{-1} \text{ Fe(II)}$ ,  $97.1 \text{ mg L}^{-1} \text{ H}_2\text{O}_2$ ; B:  $13.3 \text{ mg L}^{-1} \text{ Fe(II)}$ ,  $143 \text{ mg L}^{-1} \text{ H}_2\text{O}_2$  and C:  $15.9 \text{ mg L}^{-1} \text{ Fe(II)}$ ,  $202 \text{ mg L}^{-1} \text{ H}_2\text{O}_2$ . pH 2.8,  $T=25^\circ\text{C}$ .

B and C were applied in the photo-Fenton process, less than  $1.2 \text{ mg L}^{-1}$  were found before the biological coupling.

The monitoring of oxalic acid evolution over 350 min showed that its production was higher for doses B and C ( $61.5 \text{ mg L}^{-1}$  and  $65.5 \text{ mg L}^{-1}$ , respectively) than for dose A ( $44.6 \text{ mg L}^{-1}$ ). Maxima in the evolution curves were achieved at the moment selected for the coupling with the biological system. Both, acetic and oxalic acid were produced after ring opening, as described before [14]. Soft oxidant conditions favour the production of acetic acid, while an increase in  $\text{OH}^\bullet$  concentration produces a higher concentration of oxalic acid, which is the product of the oxidation of acetic acid.

Formic acid can be generated from the direct oxidation of methyl groups or from oxalic or acetic acid oxidation [15]. At 60 min, the formic acid concentration of effluents treated with doses B and C was approximately  $25 \text{ mg L}^{-1}$ , while the concentration for effluent treated with dose A was  $22.5 \text{ mg L}^{-1}$ . High concentration of formic acid remained in solution after 350 min when the polluted effluent was treated with photo-Fenton dose A (i.e.,  $27 \text{ mg L}^{-1}$ ), thus suggesting that formic acid is more resistant to degradation than acetic or oxalic acid. On the other hand, when the effluent was treated with doses B or C, due to the higher  $\text{OH}^\bullet$  concentration used, formic acid concentration decrease to  $13.8 \text{ mg L}^{-1}$  and  $11.2 \text{ mg L}^{-1}$ , respectively.

Short acids percentages at the end of photo-Fenton process are represented in Fig. 6. The 100% value corresponds to the residual TOC present in solution after 60 min of photo treatment and the value of carbon content in the form of short acids is calculated according to this percentage. The figure also shows the existence of non-identified organic matter (NIOM) for the three treated effluents. In order to understand differences between biodegradability at the end of the chemical process UPLC/MS (RP), GS/MS and HPLC(HILIC)/MS were used in an attempt to characterize the NIOM.

According to the results on the chloride, nitrogen, and short acid release, it could be infer that a part of the identified organic

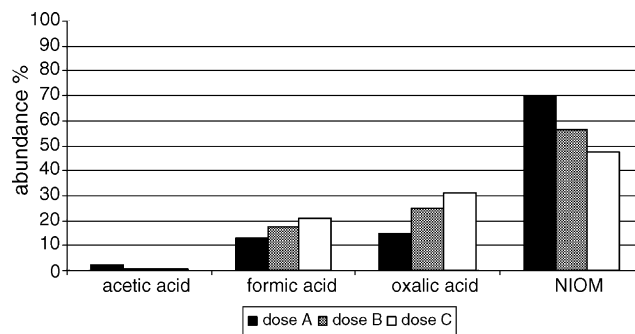


Fig. 6. Relative abundance of different acids and non-identified organic matter (NIOM) after 60 min of irradiation of Diuron and Linuron with A, B and C reagent doses. A:  $9.25 \text{ mg L}^{-1}$  Fe(II),  $97.1 \text{ mg L}^{-1}$   $\text{H}_2\text{O}_2$ ; B:  $13.3 \text{ mg L}^{-1}$  Fe(II),  $143 \text{ mg L}^{-1}$   $\text{H}_2\text{O}_2$  and C:  $15.9 \text{ mg L}^{-1}$  Fe(II),  $202 \text{ mg L}^{-1}$   $\text{H}_2\text{O}_2$ . pH 2.8,  $T=25^\circ\text{C}$ .

compounds present after 60 min contain chlorine in the case A and nitrogen for the three cases A, B and C.

### 3.3. Identification of first by-products formed and degradation mechanism

The photoproducts formed in the first steps of the oxidation process of Diuron and Linuron herbicides when A, B and C photo-Fenton reagent doses were used were investigated by means of UPLC(RP)–MS (see Fig. 7 for UPLC chromatogram). The short column employed in the UPLC technique enabled the identification of unstable products. Ten products were identified by the molecular ions and mass fragment ions detected at the MS. The structures of the by-products as well as the main fragmentations are summarized in Table 1. In addition, initial compounds (Linuron and Diuron) were also found in the chromatogram (i.e., compounds 6 and 10).

Due to the characteristic isotopic distribution of the presence of chloride atoms in a molecule ( $\text{Cl}^{35}$  and  $\text{Cl}^{37}$ ), it can be

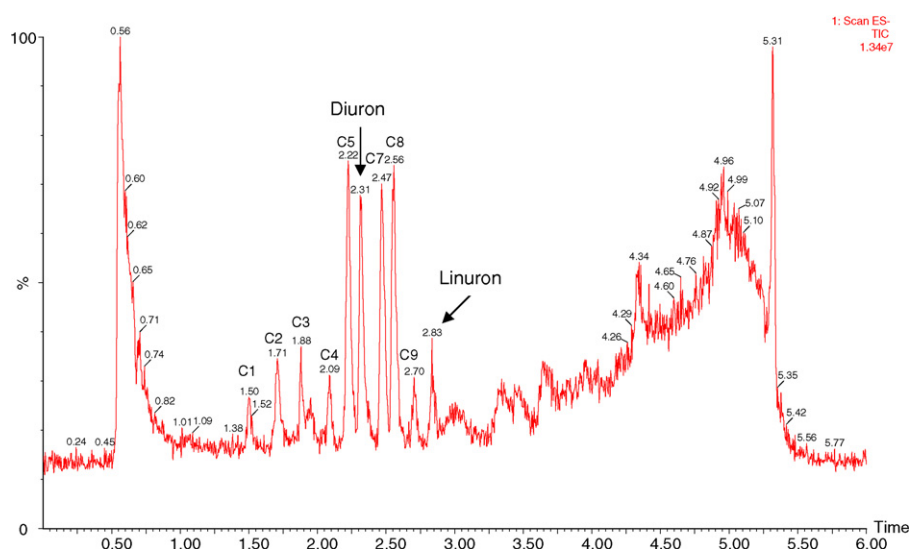


Fig. 7. UPLC chromatogram in scan mode obtained at 25 V and corresponding to 15 min of an experiment of photo-Fenton with reactant dose A ( $9.25 \text{ mg L}^{-1}$  Fe(II),  $97.1 \text{ mg L}^{-1}$   $\text{H}_2\text{O}_2$ ).

Table 1  
Main fragments arising from MS analysis of Diuron and Linuron degradation samples

Compound	Retention time (min)	Molecular weight ( <i>m/z</i> )	Molecular ion and fragmentations	Photoproduct
1	1.50	220	219(100), 176 (22)	
2	1.71	250	249 (5), 203 (100), 160 (5)	
3	1.88	248	247 (7), 217 (100), 160 (68)	
4	2.09	264	263 (8), 217 (100), 160 (23)	
5	2.22	248	247 (25), 202 (100)	
6 (Diuron)	2.31	232	231	
7, 8	2.47, 2.55	264	263 (20), 202 (100)	

Table 1 (Continued)

Compound	Retention time (min)	Molecular weight ( <i>m/z</i> )	Molecular ion and fragmentations	Photoproduct
9	2.70	246	245 (100), 217 (30), 188 (52), 160 (28)	
10 (Linuron)	2.83	248	247	

confirmed the presence of two chloride atoms in all the structures determined (i.e., three peaks with isotopic abundance 100%, 66% and 10.6%). Moreover, no recombination between by-products formed has been observed. By interpreting the mass spectra, compound 3: *N'*-(3,4-dichlorophenyl)-*N*-(hydroxymethyl)-*N*-methyl-urea, and compound 4: *N'*-(3,4-dichlorophenyl)-*N*-(dihydroxymethyl)-*N*-methyl-urea, were identified as the products formed by the first and second attack of OH• to the methyl group of Diuron, respectively. Compound 2: *N*-(3,4-dichlorophenyl)-*N'*-(dihydroxymethyl)-urea was identified as the product formed by the attack of OH• to the second methyl group of Diuron once the first methyl group had been eliminated. This demethylation process has been proposed previously and occurs through the formation of hydroxylated or carboxylated compounds as follows [14]:



Compound 9: *N'*-(3,4-dichlorophenyl)-*N*-formyl-*N*-methyl-urea was identified as the oxidation product of compound 4. Compound 5: *N'*-(3,4-dichlorophenyl)-*N*-formoxy-urea, was the result of oxidation of Linuron with the elimination of a methyl group. Compounds 7 and 8, that show the same spectra, were identified as the products of the oxidation of compound 5 (see Fig. 8 for mass spectrum of compounds 5, 7 and 8). No explanation has been found to explain the difference in retention time. The fragment at *m/z* = 202 obtained in MS spectra of compounds 5, 7 and 8 can be explained assuming the formation of a radical anion during the fragmentation process in the electro-spray. In compounds 5, 7 and 8 NH–O–COOH and NH–O–CHO bond were present at the end of the molecule. It can be supposed that in the fragmentation process, the hydrogen atom bonded to the nitrogen atom can be transferred producing the loss of H<sub>2</sub>O and CO<sub>2</sub> on the one hand, and H<sub>2</sub>O and CO on the other. In those cases Katsumata et al. [16] and Tahmasseb et al. [20] suggest the first attack of OH• radical in the oxomethyl group of Linuron. Then, OH• attacks the methyl group after eliminate the oxomethyl group of parent compound. This assumption is contrary to our results.

Finally, compound 1 appears to be the product of hydroxyl addition to the benzene ring of the target compounds, once the methyl or hydroxymethyl groups had been eliminated. All the results, except those for compounds 5, 7 and 8, are consistent with previous publications where the presence of two main sites of initial attack by OH• radical in these kinds of compounds was suggested: the aromatic ring and the methyl group [12,14,16].

Two different compounds were found in short reaction time experiment A GC–MS analysis was carried out after 15 min of photo-Fenton process using reagent dose A. 3,4-dichloroaniline and 3,4-dichlorophenyl isocyanate were identified by the mass of the molecule and fragment ions and also, through comparison

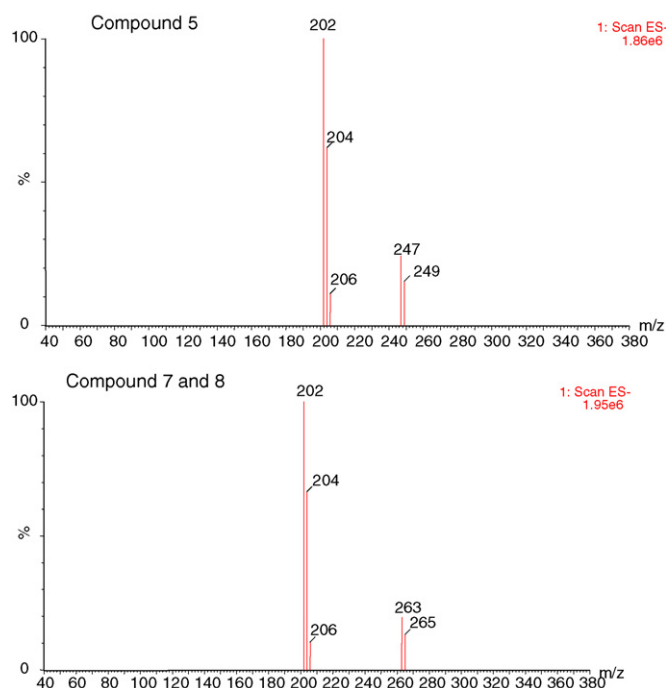


Fig. 8. LC–ESI–MS spectrum of compounds 5, 7 and 8 (Table 1).

with Wiley library data with similarities up to 86%. Katsumata et al. [16] observed 3,4-dichlorophenyl isocyanate in the degradation pathway of Linuron. Moreover, 3,4-dichloroaniline and 3,4-dichlorophenyl isocyanate were also proposed as the main degradation intermediates by Salvestrini et al. [17] in Diuron kinetic studies. These two compounds were no longer detected after 60 min of irradiation time for dose A. Multi residual monitoring (MRM) without concentrating the samples was used to detect the evolution of the first by-products formed during photo-Fenton reaction. Fig. 9 shows the relative evolution of by-products when dose A was used in the oxidation process. The kinetic behaviour of the detected by-products clearly confirms that these aromatic compounds undergo further transformation since the concentration at 60 min was negligible. Moreover, from Fig. 9 it appears that the oxidation and decarboxilation processes that eliminate alkyl groups seem more favoured than the attack to the aromatic ring by  $\text{OH}^\bullet$  radicals.

Samples at 60 min of irradiation time were concentrated by means of solid phase extraction on  $\text{C}_{18}$  cartridges and some traces of compounds 1–10 were found. Traces of the intermediates resist the  $\text{OH}^\bullet$  attack as expected at the end of a mineralization process. Similar results were obtained when effluent treated with doses B and C were investigated.

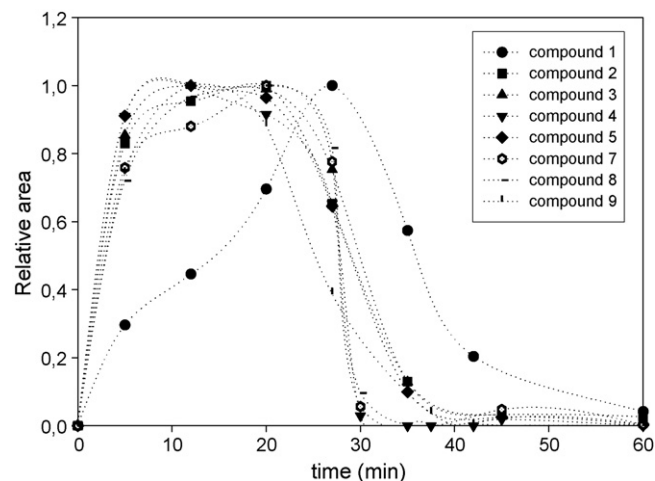
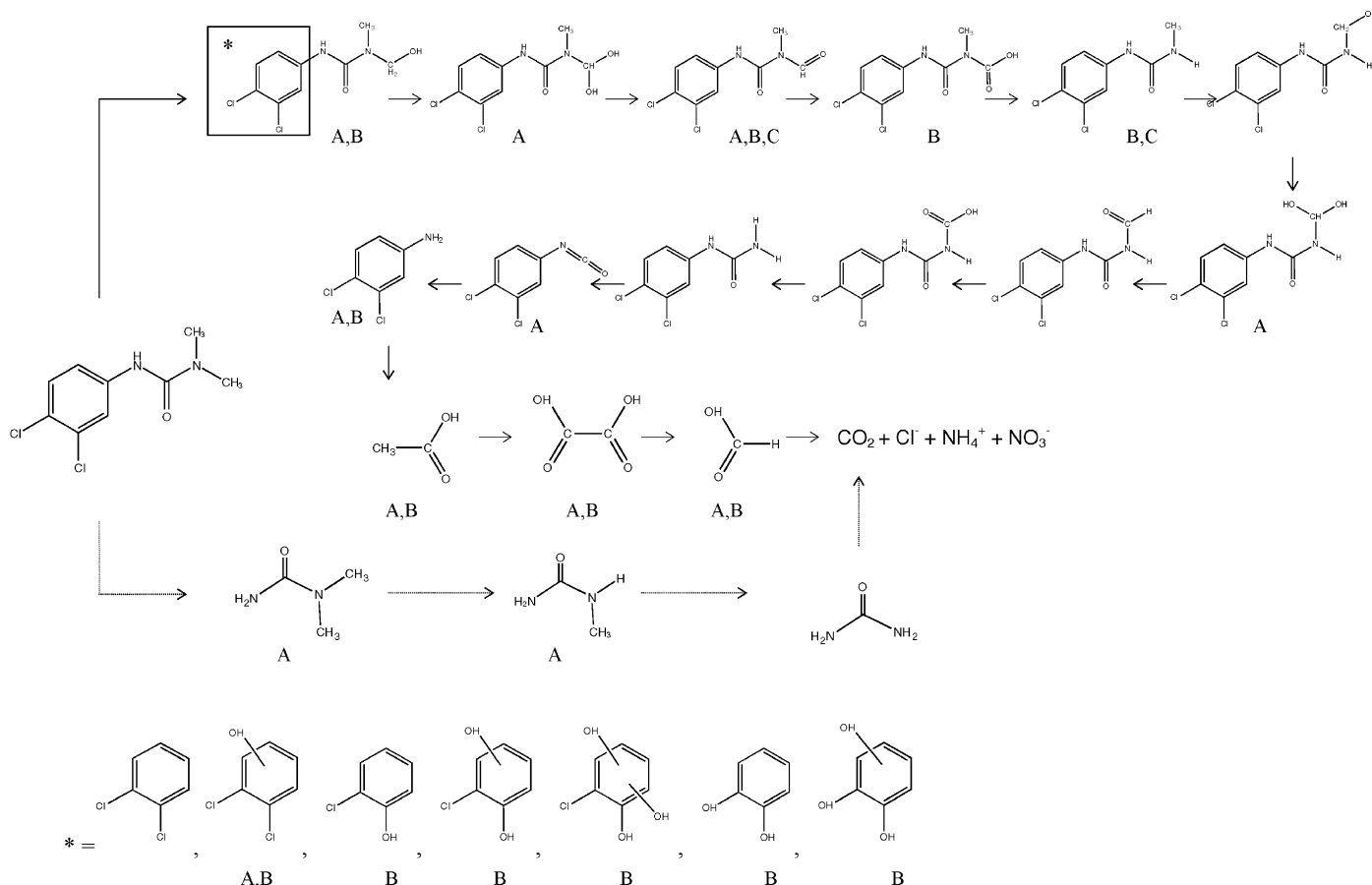


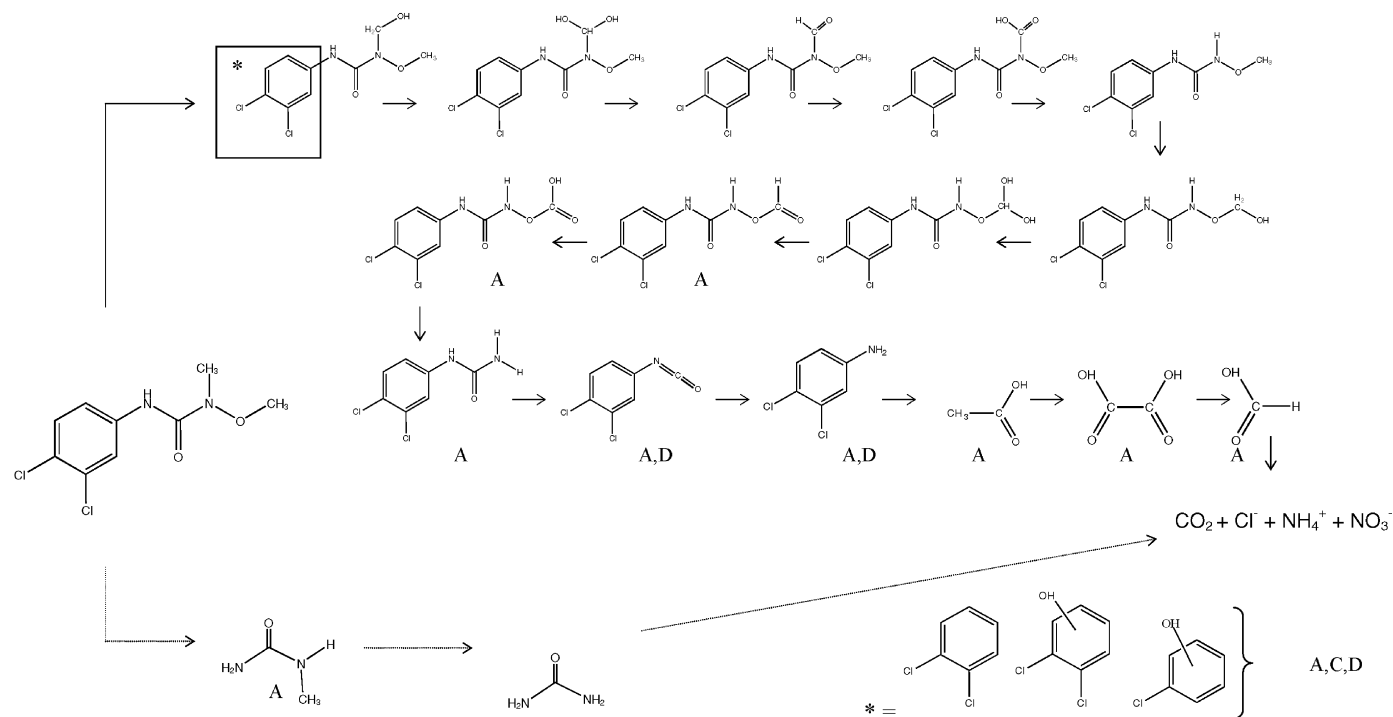
Fig. 9. Relative first by-products evolution during photo-Fenton degradation of Diuron and Linuron herbicides with dose A ( $9.25 \text{ mg L}^{-1} \text{ Fe(II)}$ ,  $97.1 \text{ mg L}^{-1} \text{ H}_2\text{O}_2$ ), pH 2.8,  $T = 25^\circ \text{C}$ .

In addition to these 13 compounds, other degradation products could exist in the photo-Fenton system. Nevertheless, they were not detected because of the high polarity of the column employed and the low concentrations used.



Scheme 1. Degradation pathways of Diuron by  $\text{OH}^\bullet$ . (A) by-products identified in this work, (B) by-products identified by Malato et al. [12] and (C) by-products identified by Tahmassebi et al. [20]. \* Radical attack to benzene ring.





Scheme 2. Degradation pathways of Linuron by OH•. (A) by-products identified in this work, (C) by-products identified by Tahmasseb et al. [20] and (D) by-products identified by Katsumata et al. [16]. \*Radical attach to benzene ring.

### 3.4. Relation between the end by-products formed and biodegradability

The differences between the organic matter present at the end of the three photo-treated effluents were investigated. Smaller and increasingly polar compounds are supposed to be generated along the oxidation process. As described in the introduction, HPLC(HILIC)/MS is the analytical technique that can correctly analyze those small polar compounds.

Differences were found when solutions treated with doses A, B and C were analyzed by means of HPLC(HILIC)/MS. Higher concentrations of methylurea, and 1,1-dimethylurea were identified in the solution treated with dose A. The isotopic distribution of methylurea peak as well as molecular mass and retention time coincided with that of an authentic standard. On the other hand, a *N,N'*-dimethylurea standard was used to determine the second product detected. Isotopic distribution as well as molecular mass coincided with the standard but retention time was different. Therefore we can consider that the methylurea formed in the degradation of parent compounds was the 1,1-dimethylurea. This assumption is in accordance with the logical order in the degradation pathway.

The percentages of these two final products generated in the oxidation process were analyzed. 100% was arbitrary assigned to the product found in photo-treated solution A, then, based on this the relative amounts in samples B and C were calculated. Methylurea present in solution B and C reach 43% and 21%, respectively. On the other hand 1,1-dimethylurea was not present in phototreated solution C, while only 5% was founded in solution B. Although urea should be present at the end of the oxidation process [18] the comparison of both, the photo-

treated solutions with a standard solution of urea indicates its absence.

Biodegradability between 27.3% and 53.1% has been determined for dimethylurea after 14 days of aerobic domestic sludge treatment [19]. This means that when this product is generated in the chemical step, a higher hydraulic retention time (HRT) in the sequencing batch reactor would be needed to completely eliminate organic matter from solution. In such a case, economic considerations should be necessary in order to give priority to stronger chemical pre-treatment or a longer secondary biological process. It should be mentioned that the presence of other by-products as methylaniline or short chlorinated compounds cannot be rejected but their presence is difficult to determine with the analytical methods used in this work. In fact no total chloride was recovered in photo-treatment of Diuron and Linuron solution with dose A as explain above. Further experiments are required in order to completely close nitrogen and carbon balances in this oxidation process. Based on the intermediate products found in this work and the results obtained by other researchers [12,16,20], an improved possible degradation pathway for Diuron and Linuron is proposed in Schemes 1 and 2, respectively.

## 4. Conclusions

The degradation of Diuron and Linuron herbicides has been carried out by means of a chemical (photo-Fenton) and a biological coupled system. Three combinations of reactant dose have been used in the chemical step. Different degrees of elimination of total organic matter have been achieved in the secondary biological treatment depending on the by-products generated in the

chemical stage. Formic, oxalic and acetic acids appear at different concentration during the photo-Fenton experiments. The presence of acetic acid has been found to be higher under soft oxidant conditions while an increase in  $\text{OH}^\bullet$  concentration produces a higher concentration of oxalic acid. 3,4-dichloroaniline and 3,4-dichlorophenyl isocyanate have been found as intermediates in the oxidation processes among other hydroxylated by-products.

The presence of methylurea and 1,1-dimethylurea as well as some non-identified chlorinated compound seem to be the cause of the different biodegradability of the photo-treated effluents.

### Acknowledgements

This work was supported by the Spanish Government (MEC, project CTQ2005-02808) and the European Commission (CADOX project, EVK1-CT-2002-00122). We also want to thank Makhteshim Agan España, S.A. for providing the Linuron herbicide.

### References

- [1] M. Pera-Titus, V. García-Molina, M.A. Baños, J. Jiménez, S. Espulgas, *Appl. Catal. B: Environ.* 47 (2004) 219–256.
- [2] V. Sarria, S. Kenfack, O. Guillod, C. Pulgarin, *J. Photochem. Photobiol. A: Chem.* 159 (2003) 89–99.
- [3] S. Parra, S. Malato, C. Pulgarín, *Appl. Catal. B: Environ.* 36 (2002) 131–144.
- [4] J. Garcia-Montaña, F. Torrades, J.A. Garcia-Hortal, X. Doménech, J. Peral, *Appl. Catal. B: Environ.* 67 (2006) 86–92.
- [5] M.J. Farré, X. Doménech, J. Peral, *Water Res.* 40 (2006) 2533–2540.
- [6] M. Kotsou, A. Kyriacou, K. Lasaridi, G. Pilidis, *Process Biochem.* 39 (2004) 1653–1660.
- [7] F. Al Momani, O. Gonzalez, C. Sans, S. Esplugas, *Water Sci. Technol.* 49 (2004) 293–298.
- [8] R. Bauer, H. Fallmann, *Res. Chem. Intermed.* 23 (1997) 341–354.
- [9] F. Haber, J. Weiss, *Proc. R. Soc. Series A* 147 (1934) 332–351.
- [10] J. Pignatello, *Environ. Sci. Technol.* 26 (1992) 944–951.
- [11] A.J. Alpert, *J. Chromatogr.* 499 (1990) 177–196.
- [12] S. Malato, J. Cáceres, A.R. Fernández-Alba, L. Piedra, M.D. Hernando, A. Agüera, J. Vidal, *Environ. Sci. Technol.* 37 (2003) 2516–2524.
- [13] L.H. Keith, W.A. Telliard, *Environ. Sci. Technol.* 13 (1979) 416–424.
- [14] L. Lhomme, S. Brosillon, D. Wolbert, J. Dussaud, *Appl. Catal. B: Environ.* 61 (2005) 227–235.
- [15] M.I. Franch, J.A. Ayllon, J. Peral, X. Doménech, *Catal. Today* 76 (2002) 221–233.
- [16] H. Katsumata, S. Kaneco, T. Suzuki, K. Ohta, Y. Yobiko, *Chem. Eng. J.* 108 (2005) 269–276.
- [17] S. Salvestrini, P. Di Cerbo, S. Capasso, *Chemosphere* 48 (2002) 69–73.
- [18] M. Hincapié, G. Peñuela, M.I. Maldonado, O. Malato, P. Fernández-Ibáñez, I. Oller, W. Gernjak, S. Malato, *Appl. Catal. B: Environ.* 64 (2006) 272–281.
- [19] OECD HPV Chemical Programme, *SID Dossiers (SIAM 17, 2003)*.
- [20] L.A. Tahmasseb, S. Nélieu, L. Kerhoas, J. Einhorn, *Sci. Total Environ.* 291 (2002) 33–44.